

## Collective multipole excitations in small metal particles: Critical angular momentum $l^{\text{cr}}$ for the existence of collective surface modes

W. Ekardt

*Solid State Division, Oak Ridge National Laboratory, Oak Ridge, Tennessee 37831  
and Fritz-Haber-Institut der Max-Planck-Gesellschaft, Faradayweg 4-6, D-1000 Berlin West 33, West Germany*

(Received 5 April 1985)

The electronic multipole response properties of small metal particles are investigated within the frame of a self-consistent spherical jellium model. The method used is the time-dependent local-density approximation (TDLDA), which was used before in a study of the dipole response [W. Ekardt, Phys. Rev. Lett. **52**, 1925 (1984)]. On comparing the TDLDA response with the response of a system of noninteracting electrons, we see clearly how the electron-electron interaction is switched off rather suddenly around a critical angular momentum  $l^{\text{cr}}$ . It is shown that the value of  $l^{\text{cr}}$  can be obtained from the equation  $q^{\text{cr}}=l^{\text{cr}}/R$ , where  $R$  is the radius of the jellium background and  $q^{\text{cr}}$  is the critical wave vector of the planar jellium surface. This result is consistent with a result found earlier for  $l=1$  [W. Ekardt, Phys. Rev. B **31**, 6360 (1985)]: A spherical surface behaves across the jellium edge like a patch of a planar jellium surface.

### I. INTRODUCTION

Quite recently a number of authors have shown<sup>1-7</sup> how the microscopic dipolar response properties of small metal particles deviate in a characteristic manner from that predicted by classical electrodynamics. The model system used in all of these investigations was the spherical jellium particle whose electronic properties in the ground state had to be studied<sup>8-10</sup> before the time-dependent local-density approximation (TDLDA) (Refs. 11 and 12) could be applied.

In the present paper we extend this kind of study to the higher multipoles mainly to see how the electron-electron interaction is increasingly less important in determining the electronic response properties. The reason why the electron-electron interaction can be expected to be switched off with an increase of  $l$  is simply the increasing inhomogeneity of all physical quantities being involved in this kind of excitation. In Fourier space this amounts to taking into account larger and larger  $k$  components of the Coulomb interaction  $4\pi/k^2$ , which drops down in this way. So the existence of a critical region of  $l$  values can be expected to occur in the same way as the existence of a critical wave vector is known to occur both for the volume modes<sup>13</sup> and for the surface modes of a planar jellium surface.<sup>14</sup>

As we know from our earlier study of the dipole response,<sup>7</sup> size-dependent damping is active as long as the collective mode is located in one or more bound-continuum transition regions. As with increasing  $l$  the number of decay channels of this kind increases more or less gently, it is an interesting question whether or not the existence of collective modes breaks down abruptly. As we shall see, this is indeed the case (*cum grano salis*) as far as the collective surface mode is concerned.

Because of the existence of Kramers-Kronig relations, connecting the real part and the imaginary part of every

kind of physical response, the same question can be studied just by looking at the  $l$  dependence of the static polarizability of a spherical jellium particle. In this respect our work is similar to the earlier work by Mahan<sup>15</sup> who calculated the static polarizability of a variety of atoms and ions up to  $l=4$ . Mahan's observations were that in the case of atoms (and atomic ions) already the static quadrupole polarizability is essentially that of a system of independent atomic electrons. The reason for this result seems to be that the  $l=2$  atomic electron-hole pairs establish an induced charge density which is already overly inhomogeneous to make the Coulomb force between various electron-hole pairs an effective coupling mechanism for collective motion. The  $l$  value, on which the independent and the dependent particle responses are more or less the same, is larger for an extended object (such as the self-consistent spherical jellium sphere) than it is for an atom; this is not surprising.

We compare our results with those of Liebsch,<sup>16</sup> who calculated the  $q_{\parallel}$  dependence of the induced charge density of a planar jellium surface with the help of the same formalism as used in the present paper.

The rest of the paper is organized as follows. Section II gives a short summary of the formalism; Sec. III contains the results concerning the static response properties; Sec. IV turns to a presentation of the dynamical response and shows how the critical angular momentum  $l_{\text{cr}}$  originates, and Sec. V is the conclusion.

### II. FORMALISM

As the application of the TDLDA (Refs. 11 and 12) to the spherical jellium particle was already described,<sup>2,7</sup> only a short summary is given here mainly to introduce our notation for the rest of the paper. Within linear response theory and with neglect of retardation, the induced charge density  $\rho_{\text{ind}}(\mathbf{r};\omega)$ , due to a frequency-

dependent external potential  $V_{\text{ex}}(\mathbf{r};\omega)$ , is determined by the retarded density-density correlation function  $\chi(\mathbf{r},\mathbf{r}';\omega)$  in the following way:

$$\rho_{\text{ind}}(\mathbf{r};\omega) = \int d\mathbf{r}' \chi(\mathbf{r},\mathbf{r}';\omega) V_{\text{ex}}(\mathbf{r}';\omega). \quad (1)$$

Here,  $\chi(\mathbf{r},\mathbf{r}';\omega)$  obeys an integral equation which can be derived by demanding the system to respond in a self-consistent manner:

$$\begin{aligned} \chi(\mathbf{r},\mathbf{r}';\omega) &= \chi^0(\mathbf{r},\mathbf{r}';\omega) \\ &+ \int \int d\mathbf{r}'' d\mathbf{r}''' \chi^0(\mathbf{r},\mathbf{r}'';\omega) \\ &\quad \times K(\mathbf{r}'',\mathbf{r}''') \chi(\mathbf{r}''',\mathbf{r}';\omega). \end{aligned} \quad (2)$$

In Eq. (2) the kernel  $K$  consists of the Coulomb interaction and an approximate description of exchange and correlation in the following way:<sup>11,12</sup>

$$K(\mathbf{r}'',\mathbf{r}''') = \frac{2}{|\mathbf{r}''-\mathbf{r}'''|} + \frac{dV_{\text{xc}}}{d\rho} \delta(\mathbf{r}''-\mathbf{r}'''), \quad (3)$$

$$\begin{aligned} \chi_l(r,r';\omega) &= \chi_l^0(r,r';\omega) + \int_0^\infty dr'' (r'')^2 \chi_l^0(r,r'';\omega) [dV_{\text{xc}}/d\rho] \chi_l(r'',r';\omega) \\ &+ \int_0^\infty dr'' (r'')^2 \int_0^\infty dr''' (r''')^2 \chi_l^0(r,r'';\omega) [4\pi/(2l+1)] B_l(r'',r''') \chi_l(r''',r';\omega), \end{aligned} \quad (5)$$

with  $B_l(r'',r''') = 2r''^l/r'''^{l+1}$ . In Eq. (5) the  $l$ th partial wave independent particle susceptibility  $\chi_l^0(r,r';\omega)$  is obtained from the general equation (4) after some angular momentum algebra in standard fashion in the following way [in Eq. (6),  $R_{l_i,n_i}(r)$  denotes the radial part of the occupied level with angular momentum quantum number  $l_i$  and with  $n_i$  being the  $n_i$ th state with  $l_i$  and an energy  $\epsilon_{l_i,n_i}$ ]:

$$\begin{aligned} \chi_l^0(r,r';\omega) &= \sum_{l_i,n_i}^{\text{occ}} \frac{1}{2\pi} R_{l_i,n_i}(r) R_{l_i,n_i}(r') (2l_i+1) \sum_{k=0}^{\min\{l,l_i\}} \frac{a_{l-k} a_k a_{l-k}}{a_{l_i+l-k}} \frac{2l_i+2l-4k+1}{2l_i+2l-2k+1} \\ &\quad \times G_{l_i+l-2k}(r,r';\epsilon_{l_i,n_i}+\omega) + \text{c.c.} \end{aligned} \quad (6)$$

$\{[\epsilon_{l_i,n_i}+\omega] \Rightarrow [\epsilon_{l_i,n_i}-\omega]\}$ . In Eq. (6) the function  $a_k = (2k-1)!!/k!$ .

Finally the  $l$ th retarded Green's function  $G_l(r,r';E)$  is obtained from two solutions of the ground state Schrödinger-like equation as follows:<sup>11</sup>

$$G_l(r,r';E) = j_l(r_<E) h_l(r_>E) / [r^2 W(j_l, h_l)]_{r=c}. \quad (7)$$

Here  $j_l$  is regular for  $r \rightarrow 0$ ,  $h_l$  fulfills the outgoing-wave boundary condition,  $W$  is the Wronskian, and  $c$  is an arbitrary constant. As both the kernel  $K$ , Eq. (3), and the independent particle susceptibility  $\chi_l^0$ , Eq. (4), are determined from the ground state Schrödinger equation, we had to solve the ground-state problem first before the TDLDA could be applied. This was done in Ref. 10 (see also Refs. 6, 8, and 9).

Once Eq. (5) is solved, the induced charge density is obtained from Eq. (1). For an external multipole potential of the form

$$V_{\text{ex}} = -r^l P_l(\cos\theta) \epsilon_l e^{-i\omega t}, \quad (8)$$

with  $P_l$  the Legendre polynomial and  $\epsilon_l$  a (small) constant, the induced charge density  $\rho_{\text{ind}}$  is given as follows:

where  $dV_{\text{xc}}/d\rho$  is the density derivative of the exchange-correlation potential in the ground state. On the other hand, the independent particle response function  $\chi^0(\mathbf{r},\mathbf{r}';\omega)$  is constructed from single-particle wave functions of the Kohn-Sham ground-state potential as follows:

$$\begin{aligned} \chi^0(\mathbf{r},\mathbf{r}';\omega) &= \sum_i^{\text{occ}} \Phi_i(\mathbf{r}) \Phi_i^*(\mathbf{r}') G(\mathbf{r},\mathbf{r}';\epsilon_i+\omega) \\ &+ \sum_i^{\text{occ}} \Phi_i^*(\mathbf{r}) \Phi_i(\mathbf{r}') G^*(\mathbf{r},\mathbf{r}';\epsilon_i-\omega). \end{aligned} \quad (4)$$

In Eq. (4), the sum is over the one-particle states occupied in the ground state  $\Phi_i$ , with energy parameter  $\epsilon_i$ , and  $G$  is the retarded Green's function in the ground-state potential.<sup>11,12</sup>

If we restrict the calculations to ground states pertaining to completely filled shells the system is spherically symmetric and, as a consequence, the response is diagonal with respect to the angular momentum  $l$ . In that case, instead of solving the general equation (4), we need to solve only the much simpler equation,<sup>1-7</sup>

$$\rho_{\text{ind}}(r,\theta;\omega) = -\epsilon_l P_l(\cos\theta) \int_0^\infty dr' (r')^{2+l} \chi_l(r,r';\omega). \quad (9)$$

From this equation, the polarizability  $\alpha_l$  can be shown to be<sup>15</sup>

$$\alpha_l(\omega) = \int_0^\infty dr r^l (-1) \frac{8\pi}{2l+1} r^2 \int_0^\infty dr' (r')^{2+l} \chi_l(r,r';\omega). \quad (10)$$

Equation (10) completes the formalism.

Whereas the dipole response function  $\alpha_{l=1}(\omega)$  is probed by single-photon experiments, the higher multipole polarizabilities can be experimentally observed either by inelastic x-ray scattering or by inelastic electron scattering. Let us work out the formula pertaining to the latter case.

An "external" electron at a position  $\mathbf{r}_e$  gives rise to the following perturbing Hamiltonian  $H'$ :

$$H' = \int d\mathbf{r} \frac{2}{|\mathbf{r}-\mathbf{r}_e|} \rho(\mathbf{r}). \quad (11)$$

Here  $\rho(\mathbf{r})$  is the charge density operator of the jellium sphere electrons. Within first-order perturbation theory the total transition probability due to  $H'$  is given by

Fermi's golden rule as follows:

$$W = 2\pi \sum_{\mathbf{k}_f} \sum_s |\langle s, \mathbf{k}_f | H' | 0, \mathbf{k}_i \rangle|^2 \delta(E_{s0} - E_{if}). \quad (12)$$

In this equation,  $|s\rangle$  is an exact, excited state of the jellium sphere;  $|0\rangle$  is its ground state,  $E_{s0} \equiv E_s - E_0$  an exci-

$$\frac{\partial^2 \sigma}{\partial E_f \partial \Omega_{\mathbf{k}_f}} = 8 \frac{k_f}{k_i} \frac{1}{\pi} \frac{1}{q^4} \sum_{l=0}^{\infty} 4\pi(2l+1) \int_0^{\infty} dr r^2 j_l(qr) \int_0^{\infty} dr' (r')^2 j_l(qr') \text{Im} \chi_l(r, r'; \omega_{if}). \quad (13)$$

In this equation,  $j_l(qr)$  is the  $l$ th spherical Bessel function and  $\text{Im}$  means the imaginary part. In forward scattering geometry we have  $q \rightarrow 0$ . Hence  $j_l$  can be expanded to first order to give an expression,

$$j_l(qr) \rightarrow \sim (qr)^l. \quad (14)$$

So it becomes clear how the various multipole polarizabilities  $\alpha_l(\omega)$ , Eq. (10), are directly experimentally accessible in forward scattering experiments of fast electrons. In the case of wide-angle scattering, which might be preferable to "separate" a certain  $l$ , the full expression Eq. (13) must be calculated.

### III. STATIC MULTIPOLE POLARIZABILITY

Classically, the  $l$ th polarizability of a particle with radius  $R$  and with bulk dielectric constant  $\epsilon(\omega)$  is given by

$$\alpha_l^{\text{cl}}(\omega) = \frac{l[\epsilon(\omega) - 1]}{l\epsilon(\omega) + l + 1} R^{2l+1}. \quad (15)$$

If the Drude dielectric constant is used for  $\epsilon(\omega)$  [which implies  $\epsilon(\omega) \rightarrow -\infty$  for  $\omega \rightarrow 0$ ], it follows

$$\alpha_l^{\text{cl}}(\omega=0)/R^{2l+1} = 1. \quad (16)$$

Quantum mechanically, a number of characteristic deviations are to be expected both due to quantum size effects (QSE) and due to the diffuse nature of the microscopic surface of the particle. Both phenomena were discussed quite recently for the dipolar response,<sup>1-7</sup> which means  $l=1$ . More pronounced differences, compared to the classical description, will occur at larger  $l$  values simply because they represent the short-wave part of the response whose correct description is intrinsically missing in the macroscopic, long-wave, classical description. Hence, a constant ratio of  $\alpha_l(\omega=0)/R^{2l+1}$  is not to be expected.

In the case of the dipolar response it is custom to rewrite the TDLDA-derived static polarizability<sup>1-7</sup> in the following way:

$$\alpha_1/R^3 = \left[ 1 + \frac{\delta_1}{R} \right]^3, \quad (17)$$

where  $\delta_1$  gives the position of the effective dipole surface of the sphere with respect to the jellium background. The main result on  $\delta_1$  was that it is very similar to but typically a little bit smaller than the corresponding value of a planar jellium surface.<sup>17</sup> Hence, the long-wavelength response of a sphere (being not overly small) could be

tation energy; and  $\mathbf{k}_i$  and  $\mathbf{k}_f$  are the, respectively, initial- and final-state wave vectors of the probing electron. Upon Fourier expanding the perturbation  $H'$  and after dividing  $W$  by the flux per incident particle, the differential cross section can be shown to be given as follows ( $q \equiv |\mathbf{k}_f - \mathbf{k}_i|$ ):

shown to be very similar to that of a planar surface.<sup>1-7</sup> Now, it is very interesting to investigate whether this is true also for the short-wave response properties which means in spherical geometry the higher  $l$  part of the response. The results are shown in the figures.

Figure 1 shows for a "sodium sphere" of 92 valence electrons the  $l$ -dependent static polarizability in units of its classical value  $R^{2l+1}$ , both for noninteracting electrons ( $\alpha_l^0$ , dashed line) and for interacting ones ( $\alpha_l$ , continuous line) for  $l$  values up to  $l=10$ . First of all, there is a tremendous reduction of the noninteracting  $l=1$  polarizability to the  $l=1$  interacting one. This is nothing else than the effect of screening. In contrast to what was found by Mahan for atoms<sup>15</sup> there is a pronounced difference between the dashed line and the continuous one even for  $l=2$  to 5. This tells us that (not surprising for an extended "atom" with  $R=18$  a.u.) screening is still effective in reducing the independent particle polarizability. Finally, for  $l=8$  and larger there is no longer any important difference between  $\alpha_l^0$  and  $\alpha_l$ . We shall come back to this  $l$  value later in this work.

The slow and gentle increase of the interacting  $\alpha_l/R^{2l+1}$  can be understood in the following way: Let us generalize Eq. (17) to higher  $l$  values by defining the apparent  $l$  pole surface of a Kohn-Sham sphere  $\delta_l$  as follows

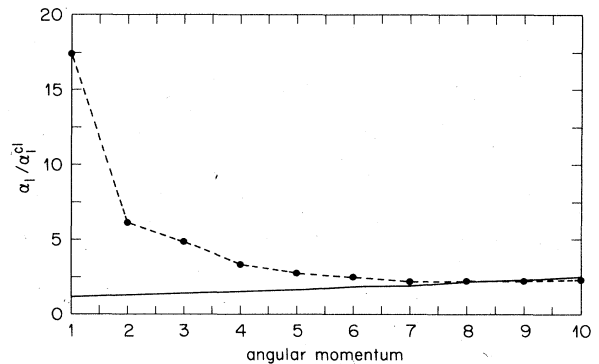


FIG. 1. Static  $l$  pole polarizability for  $N=92$  and  $r_s=4$ , which corresponds to  $R=18.057$  a.u., for  $l=1$  to  $l=10$ . Continuous line: TDLDA result, Eq. (10) of the text for  $\omega=0$ . Dashed line: Noninteracting electron result, that means  $\chi_l^0$  is used instead of  $\chi_l$  in calculating  $\alpha_l$  via Eq. (10). Both polarizabilities are given in units of the classical electrostatics result,  $\alpha_l^{\text{cl}} = R^{2l+1}$ . Due to the very effective screening at low  $l$  values there is a big difference between  $\alpha_l$  and  $\alpha_l^0$  for  $l \approx 1$  to 4. Screening is more or less ineffective beyond  $l=8$ .

$$\alpha_l/R^{2l+1} = \left[ 1 + \frac{\delta_l}{R} \right]^{2l+1} \quad (18)$$

In Fig. 2,  $\delta_l$  is shown (in a.u.) along with the ratio  $\alpha_l/R^{2l+1}$ . Except for little QSE-induced fluctuations  $\delta_l$  decreases very smoothly and seems to settle down at  $\sim 0.65$  a.u. above  $l=8$ . So, we have the important result that the  $l$ -dependent apparent surface is moving inward and that even for high  $l$  values the effective surface of the sphere is located *in front* of the jellium background. On the basis of the results obtained, we can *define* an  $l$ -dependent effective static dielectric constant in the following way:

$$\alpha_l(\omega=0) = \frac{l(\epsilon_l^{\text{eff}} - 1)}{l\epsilon_l^{\text{eff}} + l + 1} R^{2l+1}, \quad (19)$$

which gives

$$\begin{aligned} \epsilon_l^{\text{eff}} &= \frac{1 + \frac{l+1}{l} \left[ 1 + \frac{\delta_l}{R} \right]^{2l+1}}{1 - \left[ 1 - \frac{\delta_l}{R} \right]^{2l+1}} \\ &\approx - \frac{1 + \frac{l+1}{l} \left[ 1 + (2l+1) \frac{\delta_l}{R} \right]}{(2l+1) \frac{\delta_l}{R}}, \end{aligned} \quad (20)$$

where the last equality is valid because of the smallness of  $\delta_l/R$  which is typically in the range of 0.035 to 0.058. This equation makes very clear how the existence of a small but finite  $\delta_l$  leads to a finite, negative dielectric constant.

To gain further insight into the static screening behavior we have investigated the  $l$  pole polarization charge density  $\alpha_l(r)$  being defined by rewriting Eq. (10) in a way similar to what we have done for  $l=1, 2, 7$

$$\alpha_l(\omega=0) = \int_0^\infty dr r^l \alpha_l(r), \quad (21)$$

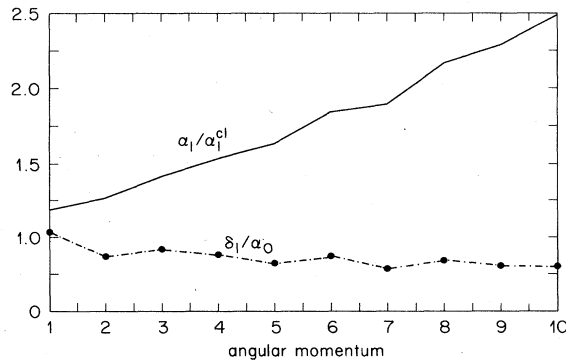


FIG. 2. Apparent  $l$  pole surface of a TDLDA sphere  $\delta_l$  defined in Eq. (18) of the text (dashed-dotted line) versus  $\alpha_l/R^{2l+1}$  (continuous line). The figure makes clear that even for large  $l$  values the apparent surface is always *in front* of the classical surface.

$$\alpha_l(r) = - \frac{8\pi}{2l+1} r^2 \int_0^\infty dr' (r')^{2+l} \chi_l(r, r'; \omega=0). \quad (22)$$

The next figures give a picture of the normalized version of  $\alpha_l(r)$ , namely the quantity

$$\tilde{\alpha}_l(r) = \alpha_l(r) / \int_0^\infty dr \alpha_l(r). \quad (23)$$

Figure 3 shows, as a reference,  $\tilde{\alpha}_1(r)$  whose size dependence was extensively discussed both by the present author in Refs. 1, 2, 4, and 7, by Beck in Ref. 3, and the Finnish group in Ref. 6. In the following figures the actual  $\tilde{\alpha}_l(r)$  (continuous line) is always compared with  $\tilde{\alpha}_1(r)$ , represented by disconnected dots. Figure 4 shows  $\tilde{\alpha}_3$  compared with  $\alpha_1$ . There is no big difference between these two except for the period of the Friedel oscillations which is getting larger for  $l=3$ . The next figure, Fig. 5, shows  $\tilde{\alpha}_5$  compared to  $\tilde{\alpha}_1$ . Now the surface charge density is already considerably smeared out. This is even more the case for  $l=7$ , shown in Fig. 6. Not only the surface charge density is decaying but also the Friedel oscillations are heavily damped and smeared out. This is shown for  $l=9$  in Fig. 7 and for  $l=10$  in Fig. 8.

The behavior seen here is qualitatively in agreement with a result obtained quite recently by Liebsch.<sup>16</sup> He studied the  $q_{||}$  dependence of the static TDLDA response of a *planar* jellium surface. The structure of the induced charge density for  $q_{||}=k_F/2$  (and  $r_s=2.07$ ) compared to  $q_{||}=0$  looks very similar to what we obtained here (see especially Fig. 1 in Ref. 16). We shall give further comments on this analogous behavior later in this work.

Before we turn to the discussion of the *dynamical* multipole response properties, let's comment briefly on the effect of other particle numbers and different  $r_s$  values. In our previous work,<sup>1,2,4,7</sup> we studied the dipolar response properties over a wide range of particle numbers. In sharp contrast to non-self-consistent models only moderate size effects were obtained within the self-consistent TDLDA calculations. This moderate size dependence has been experimentally confirmed quite recently by Knight *et al.*<sup>18</sup> Because the higher multipoles,  $l > 1$ , correspond in wave-vector space larger  $q$  values, size effects are expected to be even weaker, and this will be

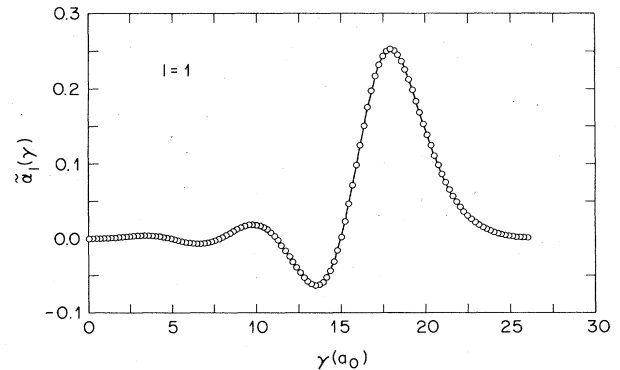


FIG. 3. Static dipole polarization charge density, normalized to 1, Eq. (23), for  $N=92$  and  $r_s=4$ . The size dependence of  $\tilde{\alpha}_1(r)$  was discussed extensively in our previous work. It is shown here as a reference for the higher  $l$  poles, shown in the subsequent figures.

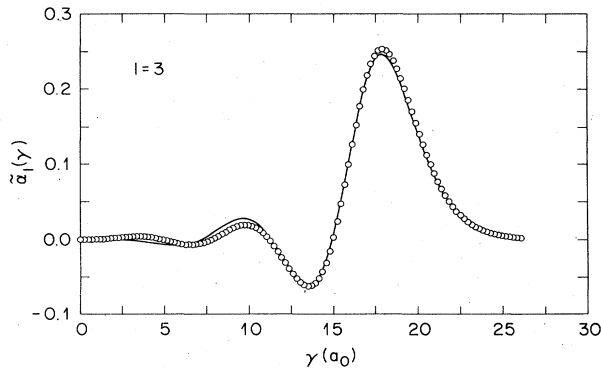


FIG. 4.  $\tilde{\alpha}_3(r)$ , continuous line, compared with  $\tilde{\alpha}_1(r)$ , dots. Nothing interesting happens except for the enlarged period of the Friedel oscillations.

verified in a separate letter. On the other hand, Beck's work<sup>3</sup> on different  $r_s$  values has made it clear that nothing special is happening if  $r_s$  is changing from 2 to 4. We think this is quite reasonable because of the similarity of the response of a spherical jellium surface and a planar one, and for the latter one we know that all the physical properties are more or less smoothly dependent on  $r_s$ .

#### IV. DYNAMICAL RESPONSE

We turn now to a discussion of the dynamical response. In our earlier work<sup>7</sup> we studied extensively the size-dependence of both the collective *surface* mode and the collective *volume* mode for the case  $l=1$ . In this paper we investigate the  $l$  dependence of the dynamical response for a jellium sphere of sodium,  $r_s=4$ , with a size  $R=18.057$  a.u. corresponding to  $N=92$  valence electrons (the uppermost filled shell in that case is the  $3s$  shell). From our earlier study for  $l=1$  we know what is to be expected when the number of particles (or the  $r_s$  value) is changed and, therefore, no other particle number or  $r_s$  value is studied in this work.

To begin with, we show in Fig. 9 a comparison of the imaginary part of  $\alpha_1(\omega)$  (continuous line) and  $\alpha_1^0(\omega)$  (dashed line) in units of  $R^3$ , for frequencies  $\omega/(\omega_p/\sqrt{3})$

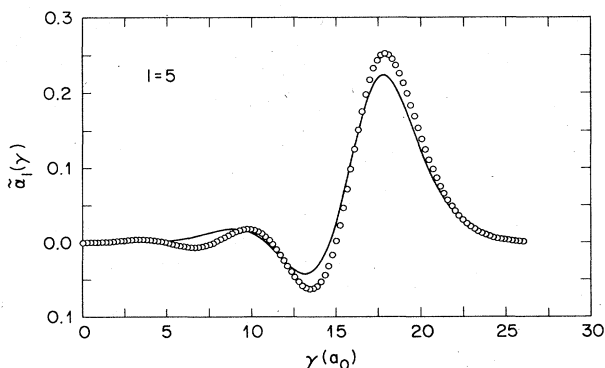


FIG. 5.  $\tilde{\alpha}_5(r)$ , continuous line, compared with  $\tilde{\alpha}_1(r)$ , dots. Now, the polarization charge density for  $l=5$  is already heavily perturbed. This figure is similar to what has been obtained quite recently for a planar jellium surface by Liebsch, Ref. 16.

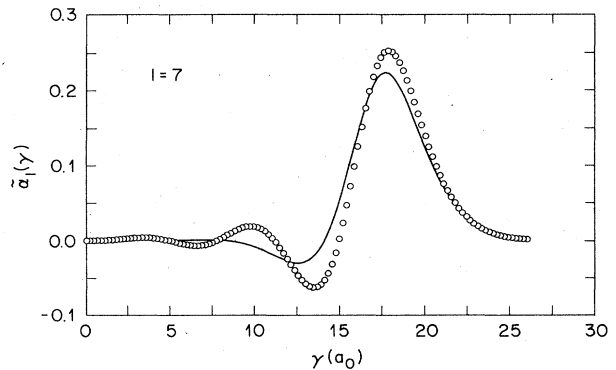


FIG. 6.  $\tilde{\alpha}_7(r)$ , continuous line, compared with  $\tilde{\alpha}_1(r)$ , dots. The Friedel oscillations are more or less destroyed. An explanation for this is possibly the growing number of terms in Eq. (6), which must be summed up to give the corresponding  $\chi_7^0$ .

from 0.4 to 2.6. The  $\text{Im}\alpha_1(\omega)$  was already published and discussed in detail in Ref. 7. It consists of numerous fine cusps which correspond to the excitation of "individual" electron-hole pairs and two collective features around 0.9 and 1.9. The former corresponds to the dipole surface plasmon whereas the latter corresponds to the (first) dipolar volume plasmon. An extensive discussion of the size dependence of this (dipole) curve and of all the points related to how to identify a certain feature as being of collective in character were already published<sup>2,4,5,7</sup> and will not be repeated here. In this paper we adopt the point of view of the Finnish group<sup>6</sup> and compare always the interacting particle response  $\alpha(\omega)$  (continuous lines) with the noninteracting particle response (dots connected by dashed lines). We see from this figure, a tremendous redistribution of oscillator strength due to the electron-electron interaction. This is nothing else than the dynamical analog to Fig. 1 where we saw how the polarizability is reduced upon the electron-electron interaction is "switched on." Oscillator strength is transferred from low-frequency excitation mainly to the new collective excitation in the region around  $\omega/\omega_s^{\text{cl}} \approx 0.9$ . This makes the

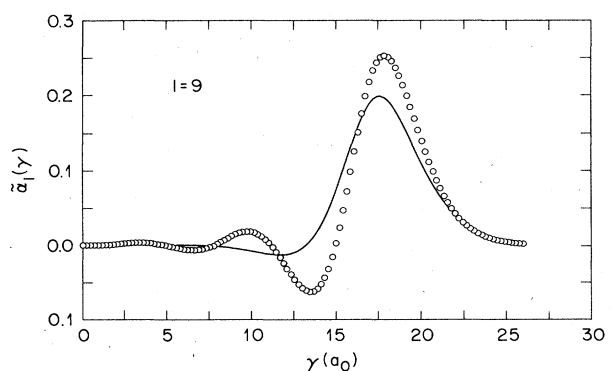


FIG. 7.  $\tilde{\alpha}_9(r)$ , continuous line, compared with  $\tilde{\alpha}_1(r)$ , dots. This should be basically the high- $l$  independent particle response, simply because there is no difference between  $\alpha_9$  and  $\alpha_9^0$  (see Fig. 1).

system "stiffer" and, consequently, less polarizable. At high frequencies these effects are, of course, unimportant. Hence  $\alpha_1(\omega)$  and  $\alpha_1^0(\omega)$  agree with each other (even for this low  $l$  value). To demonstrate this, we show in Fig. 10 the corresponding real part of the dipolar response of the system. Figure 10, together with Fig. 9, shows that at high frequencies there is indeed perfect agreement be-

tween  $\alpha_1(\omega)$  and  $\alpha_1^0(\omega)$ .

Before we go on to discuss the higher  $l$  poles, let us show shortly that, of course, both  $\alpha_1(\omega)$  and  $\alpha_1^0(\omega)$  agree, for  $\omega \rightarrow \infty$ , with the *classical* result obtained with the help of Drude's dielectric constant. The starting point of that proof is the leading term in the high-frequency expansion of the exact density-density correlation function,

$$\begin{aligned} \chi(\mathbf{r}, \mathbf{r}'; \omega) &= \sum_s \left[ \frac{\langle 0 | \rho(\mathbf{r}) | s \rangle \langle s | \rho(\mathbf{r}') | 0 \rangle}{\omega + i\delta - (E_s - E_0)} - \frac{\langle 0 | \rho(\mathbf{r}') | s \rangle \langle s | \rho(\mathbf{r}) | 0 \rangle}{\omega + i\delta + (E_s - E_0)} \right] \\ &\Rightarrow (\omega + i\delta)^{-2} \langle 0 | [[\rho(\mathbf{r}), H], \rho(\mathbf{r}')] | 0 \rangle + O(\omega^{-4}). \end{aligned} \quad (24)$$

Using some operator algebra, the last expression can be shown to be

$$\begin{aligned} \chi(\mathbf{r}, \mathbf{r}'; \omega) &\Rightarrow -(\omega + i\delta)^{-2} e^2 / m \\ &\times \{ \rho_0(\mathbf{r}) \Delta_r \delta(\mathbf{r} - \mathbf{r}') + \nabla \rho_0(\mathbf{r}) \cdot \nabla_r \delta(\mathbf{r} - \mathbf{r}') \}. \end{aligned} \quad (25)$$

In this expression  $\rho_0(\mathbf{r})$  is the density of interacting electrons in the ground state. Because of the spherical symmetry of the problem under discussion,  $\rho_0(\mathbf{r}) = \rho_0(r)$ , and an angular momentum decomposition can be applied to Eq. (25). This gives us for the dipole part of  $\chi$  the following;

$$\begin{aligned} \chi_1(r, r'; \omega) &\Rightarrow -(\omega + i\delta)^{-2} e^2 / m \\ &\times \left[ \rho_0(r) \left( \frac{\partial^2}{\partial r^2} + \frac{2}{r} \frac{\partial}{\partial r} - \frac{2}{r^2} \right) \frac{1}{r^2} \delta(r - r') \right. \\ &\left. + \frac{\partial \rho_0(r)}{\partial r} \frac{\partial}{\partial r} \frac{1}{r^2} \delta(r - r') \right]. \end{aligned} \quad (26)$$

This expression for  $\chi_1(r, r'; \omega)$ , inserted into Eq. (22) for the dipolar polarization charge density, results in

$$\alpha_1(r; \omega) \Rightarrow \frac{1}{(\omega + i\delta)^2} \frac{e^2}{m} \frac{4\pi}{3} r^2 \frac{\partial \rho_0(r)}{\partial r}. \quad (27)$$

Therefore, we obtain the following expression for the high-frequency dipolar polarizability:

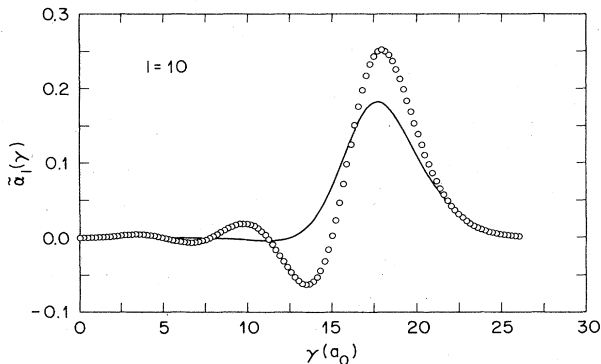


FIG. 8. The same as Fig. 7, but for  $l=10$ .

$$\begin{aligned} \alpha_1(\omega) &= \int_0^\infty dr r \alpha_1(r; \omega) \\ &\Rightarrow (\omega + i\delta)^{-2} \frac{e^2}{m} \frac{4\pi}{3} \int_0^\infty dr r^3 \frac{\partial \rho_0(r)}{\partial r} \\ &= -\frac{1}{(\omega + i\delta)^2} \frac{4\pi n_0 e^2}{m} \frac{R^3}{m} \equiv -R^3 \left[ \frac{\omega_s^{\text{cl}}}{\omega + i\delta} \right]^2. \end{aligned} \quad (28)$$

Now it is an easy task to show that, starting with the *classical* expression for  $\alpha_1$ ,

$$\alpha_1^{\text{cl}}(\omega) = R^3 \frac{\epsilon(\omega) - 1}{\epsilon(\omega) + 2}, \quad (29)$$

and using the Drude dielectric function, Eq. (28) is indeed agreeing with the classical high frequency behavior, Q.E.D.

We continue with the discussion of the higher multipole response properties. Because of the time consuming numerical work we had to do, the results are shown only in a restricted frequency region where the collective surface mode can be expected to occur. So, the curves do not

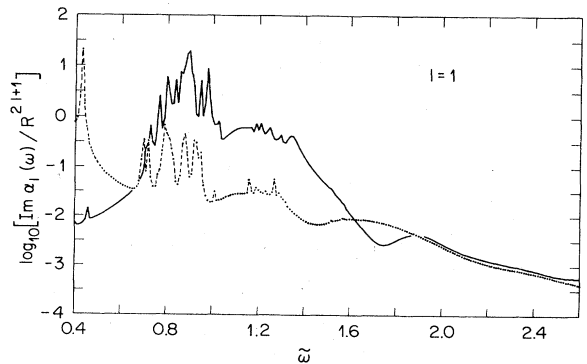


FIG. 9.  $\text{Im} \alpha_1(\omega) / R^3$ , continuous line, versus  $\text{Im} \alpha_1^0(\omega) / R^3$ , dashed line, for frequencies  $0.4 < \tilde{\omega} < 2.6$ . Here,  $\tilde{\omega} = \omega / (\omega_p / \sqrt{3})$ . The particle number is  $N=92$  and  $r_s=4$ . The physics and the size dependence of the continuous line were extensively discussed in our previous work, especially in Refs. 2 and 7. This curve is shown here as a reference. On comparing  $\alpha_1^0(\omega)$  with  $\alpha_1(\omega)$  the formation of collective motion (at the cost of low-frequency-pair motion) can clearly be seen. This is the dynamical analog to the enormous difference in the static polarizabilities  $\alpha_1$  and  $\alpha_1^0$  shown in Fig. 1.

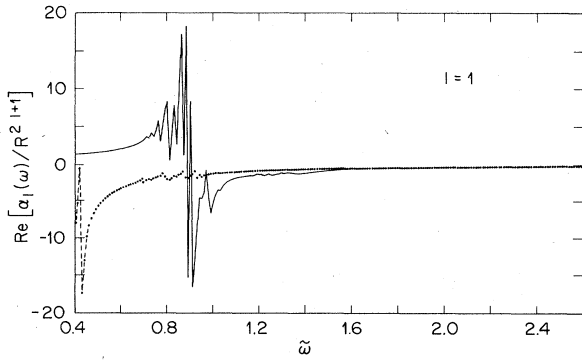


FIG. 10. The same as Fig. 9, but for the real part of the dynamical polarizability.

start at  $\omega=0$  but at  $\tilde{\omega} \equiv \omega/\omega_s^{\text{cl}}(l=1)=0.8$  where  $\omega_s^{\text{cl}}(l=1)=\omega_p/\sqrt{3}$ . The frequency  $\tilde{\omega}$  is scanned in steps of 0.01 which is obviously sufficiently fine to catch all the important features. The calculated points are then connected (as eye guide lines) with a continuous line (interacting spectrum) or by a dashed line (noninteracting spectrum).

In the classical description of a metallic sphere, based on Eq. (15) with the use of the Drude dielectric constant  $\epsilon(\omega)=1-\omega_p^2/(\omega+i0^+)^2$ , the collective  $l$  pole is located at the frequency

$$\omega_l^{\text{cl}} = \omega_p / \left[ \frac{l+1}{l} + 1 \right]^{1/2}. \quad (30)$$

This means that for  $l \rightarrow \infty$ , a spherical surface behaves as a planar one ( $\omega_\infty^{\text{cl}} = \omega_p/\sqrt{2}$ ). This result is not surprising because  $l \rightarrow \infty$  corresponds to a wavelength going down to zero, and for this case any finite curvature,  $1/R$ , is negligible. But, as we have already mentioned, this classical result is meaningless because large  $l$  values are definitely beyond the scope of the classical, macroscopic description. In a truly microscopic theory, a breakdown of collective surface motion is expected to occur in a similar way as it

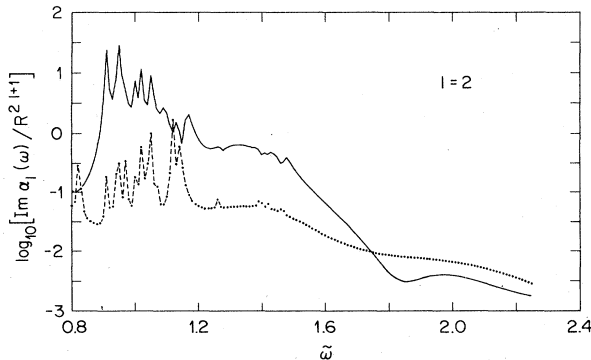


FIG. 11.  $\text{Im}\alpha_2(\omega)/R^5$ , continuous line, versus  $\text{Im}\alpha_2^0(\omega)/R^5$ , dashed line, for frequencies  $0.8 < \tilde{\omega} < 2.25$ . This is the frequency region where collective motion is expected to occur. Similar to the  $l=1$  case, there is a big difference between dependent and independent particle response. This is not surprising for low values of  $l$  because, as it is argued in the text, low  $l$  values correspond to long wavelength.

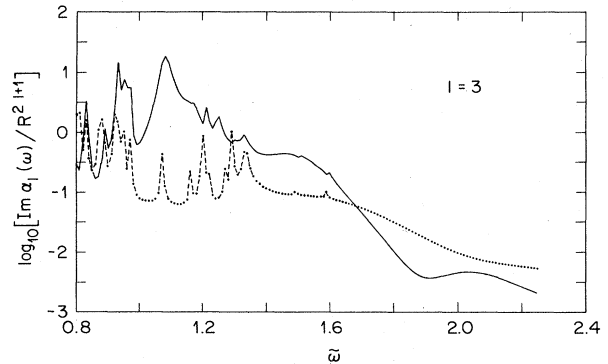


FIG. 12. The same as Fig. 11, but for  $l=3$ . The collective surface mode is around  $\tilde{\omega} \approx 1.08$ .

is known for a planar surface.<sup>14</sup> This means a transition region of critical  $l$  values should exist for which the collective  $l$  pole motion starts losing its meaning. We know from the work of Ingelsfield and Wikborg<sup>14</sup> that the critical  $q_{\parallel}$  value of a planar surface is similar to the critical  $q$  value of the bulk plasmon<sup>13</sup> despite the fact that surface-induced coupling of electron-hole pairs and collective surface modes occurs for all  $q_{\parallel}$  values down to zero.<sup>14</sup> The important result of his study is that at  $q_{\parallel}^{\text{cr}} \approx q^{\text{cr}}$  damping is increased dramatically (see Fig. 1 in Ref. 14).

From the comparison of the  $l$  pole static polarizabilities for interacting electrons and for noninteracting ones shown in Fig. 1 for  $r_s=4$  and  $N=92$  we can conclude that around  $l^{\text{cr}}=7$  or 8 collective motion gets lost. This is for the simple fact that  $\alpha_l$  approximately equals  $\alpha_l^0$ .

There is another reason why around this  $l$  value a breakdown of collective surface motion is to be expected. An  $l$  pole surface excitation has a wavelength which is approximately given by  $\lambda_l \approx 2\pi R/l$ . This is so because a surface excitation is localized in the surface region of the sphere and  $R$  can be considered as being a typical value for this. Consequently, the corresponding wave vector of this excitation is  $q_l \approx l/R$ . Now, as we have argued earlier, for a short wavelength the curvature  $1/R$  seems to be unimportant simply because  $\lambda_l/2\pi R = 1/l \rightarrow 0$ . Hence, the spherical surface is expected to behave like a planar surface. But for the latter case we know<sup>14</sup> that  $q_{\parallel}^{\text{cr}} \approx q^{\text{cr}}$ . Within the random-phase approximation (RPA),<sup>13</sup>

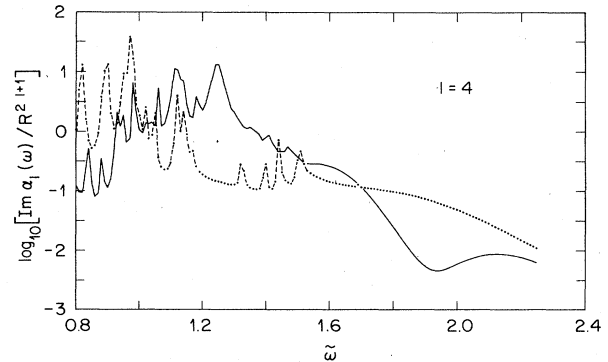


FIG. 13. The same as Fig. 11, but for  $l=4$ . The collective surface mode is around  $\tilde{\omega} \approx 1.24$ .

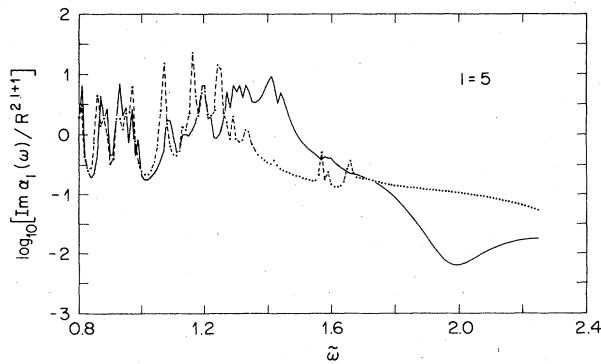


FIG. 14. The same as Fig. 11, but for  $l=5$ . The collective surface mode is around  $\tilde{\omega} \approx 1.41$ . For  $l=5$  the two spectra start agreeing with each other.

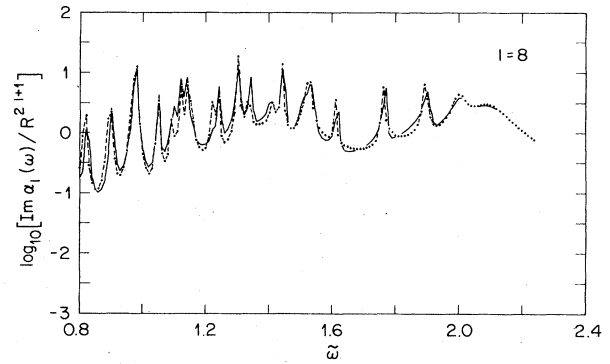


FIG. 17. The same as Fig. 11, but for  $l=8$ . Both curves agree, more or less, with each other. The electron-electron interaction is no longer determining the electronic response properties. The  $l$  value of 8 for  $N=92$  and  $r_s=4$  can be "predicted" by Eq. (33) of the text.

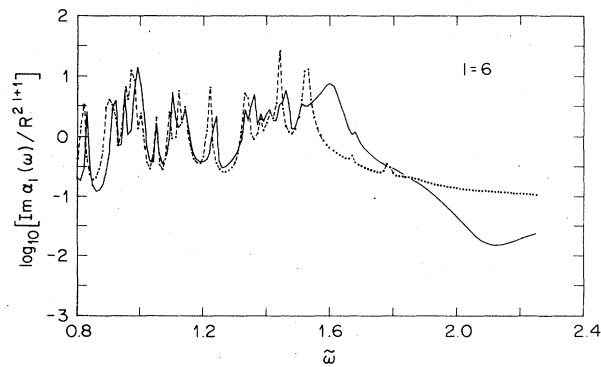


FIG. 15. The same as Fig. 11, but for  $l=6$ . The collective surface mode is around  $\tilde{\omega} \approx 1.6$ . The agreement between  $\alpha(\omega)$  and  $\alpha^0(\omega)$  is more and more increasing.

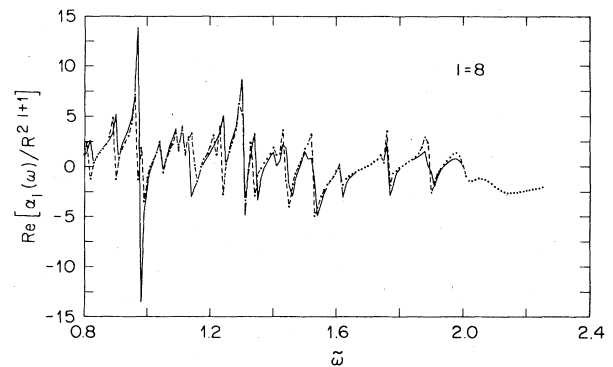


FIG. 18. To convince the conservative reader this figure shows the corresponding real part of the dynamical polarizabilities for  $l=8$ .

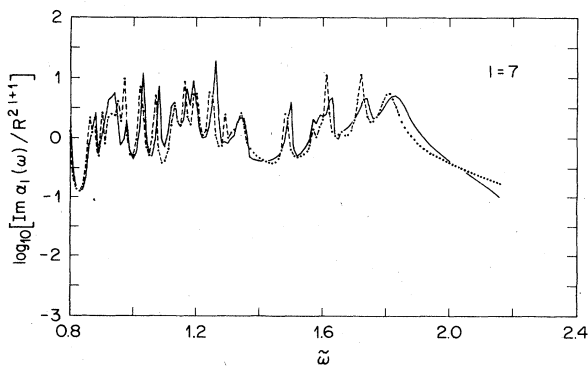


FIG. 16. The same as Fig. 11, but for  $l=7$ . In this figure it is actually no longer possible to identify a collective surface mode.

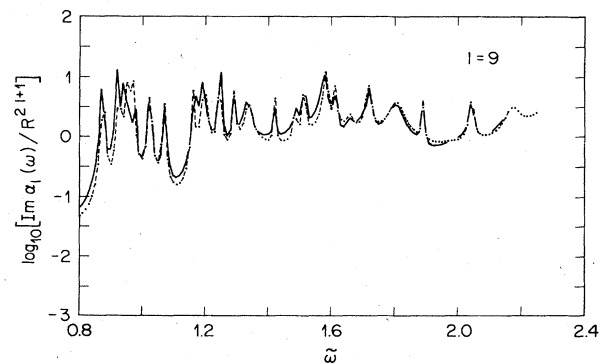
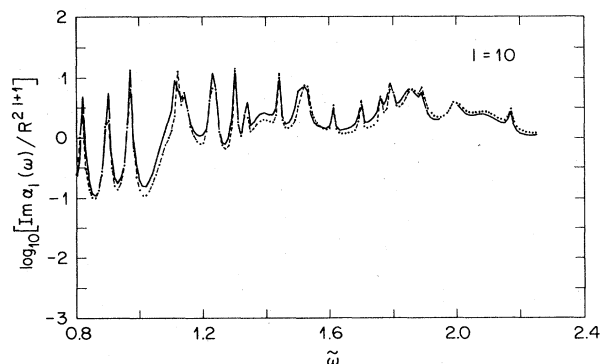


FIG. 19. The same as Fig. 11, but for  $l=9$ .

FIG. 20. The same as Fig. 11, but for  $l=10$ .

$$q^{\text{cr}} \approx \omega_p / V_F \approx 0.9 / (r_s)^{1/2}. \quad (31)$$

This means  $q^{\text{cr}} \approx 0.45$  for  $r_s=4$ , the case under study. Defining a critical angular momentum  $l^{\text{cr}}$  via

$$l^{\text{cr}} = Rq_l^{\text{cr}} \approx Rq_{\parallel}^{\text{cr}} \approx Rq^{\text{cr}},$$

and after inserting Eq. (31) for  $q^{\text{cr}}$  we arrive at

$$l^{\text{cr}} \approx 0.9R / (r_s)^{1/2}. \quad (32)$$

As in the spherical jellium model, the jellium background radius  $R$  and the particle number  $N$  are related by the equation

$$R = N^{1/3} r_s;$$

we get the final result in the form

$$l^{\text{cr}}(N) = 0.9N^{1/3} (r_s)^{1/2}. \quad (33)$$

For the case under study,  $N=92$  and  $r_s=4$ , we get  $l^{\text{cr}}=8.125 \approx 8$ . We now look at what is happening with our TDLDA-response functions.<sup>19</sup> Figure 11 shows the results for  $l=2$ . We observe similar behavior as for  $l=1$ , a large transfer of oscillator strength with a collective surface pole around  $\tilde{\omega} \approx 0.95$ . This identification can be made by means of the considerations discussed in detail in Ref. 7. For  $l=3$  (Fig. 12) no principal change occurs. The collective surface pole is shifted to  $\sim 1.08$  and is considerably broadened. Figure 13 shows the result for  $l=4$ . The collective surface pole is now at  $\sim 1.24$ . We observe still considerable redistribution of single-pair oscillator strength to the collective region. At  $l=5$ , seen in Fig. 14, the situation starts changing. One part of the spectrum looks very similar for interacting and noninteracting electrons whereas another part does not. The oscillator strength being transferred to the collective pole around  $\tilde{\omega}=1.4$  seems to come mainly from low-frequency excitations (not shown in this figure). For  $l=6$  (Fig. 15) we ob-

serve still a broad collective surface hump at  $\tilde{\omega}=1.6$ , whereas for a wide frequency region there is nearly a one-to-one correspondence between peaks observed in  $\alpha(\omega)$  and in  $\alpha_0(\omega)$ . For  $l=7$ , seen in Fig. 16, it is actually no longer possible to identify a collective surface feature though it is tempting (for the sake of continuity) to declare the broad peak around  $\tilde{\omega} \sim 1.82$  as being partly collective (simply because its width is considerably larger than the corresponding feature in the noninteracting spectrum). Finally for  $l=8$ , shown in Fig. 17, there is more or less perfect agreement between  $\text{Im}\alpha(\omega)$  and  $\text{Im}\alpha_0(\omega)$ , and this is exactly the  $l^{\text{cr}}$  value we have derived above in a somewhat heuristic manner. To convince the conservative reader, we show in Fig. 18 the corresponding real part of the response function which reveals only small differences between  $\text{Re}\alpha(\omega)$  and  $\text{Re}\alpha_0(\omega)$ . This tells us that, of course, the Coulomb interaction is still there but it is not sufficiently strong to produce new spectral features. To complete this picture we show in Figs. 19 and 20 the corresponding results for  $l=9$  and 10.

## V. CONCLUSION

Collective multipole motion has been investigated within the frame of the TDLDA with 92 valence electrons of sodium as an example. We have found that a critical angular momentum for the formation of surface plasmons does exist in very much the same manner as it is known to occur for the  $q_{\parallel}$  dependence of the surface plasmon at a planar metal surface. It has been shown that, starting with the equation  $l^{\text{cr}} = q^{\text{cr}} R$ , the critical angular momentum at a given number of valence electrons  $N$  for a bulk density of  $r_s$  is determined by

$$l^{\text{cr}}(N, r_s) = 0.9N^{1/3} (r_s)^{1/2}.$$

For the time being no experimental data seems to exist with which we could compare our predictions. However, we think that in the near future experimental data will be available at least for the static  $l$  pole polarizabilities. It is hoped that these data will agree with our theoretical predictions in the same way as it was found earlier for the dipole case.<sup>2,18</sup>

## ACKNOWLEDGMENTS

The author thanks Professor Dr. E. Zeitler for continuing interest and support. Special thanks are due to the staff of the ZIB, Berlin, for the opportunity to do these calculations on a Cray computer. Research support is acknowledged from G. D. Mahan from the University of Tennessee—Oak Ridge National Laboratory Distinguished Scientist Program. Finally, many thanks are due to my colleague, J. K. Sass, for numerous discussions on the various aspects of surface optical response.

<sup>1</sup>W. Ekardt, Ber. Bunsenges. Phys. Chem. **88**, 289 (1984).

<sup>2</sup>W. Ekardt, Phys. Rev. Lett. **52**, 1925 (1984).

<sup>3</sup>D. E. Beck, Phys. Rev. B **30**, 6935 (1984).

<sup>4</sup>W. Ekardt, Surf. Sci. **152/153**, 180 (1985).

<sup>5</sup>W. Ekardt, Solid State Commun. **54**, 83 (1985).

<sup>6</sup>M. J. Puska, R. M. Nieminen, and M. Manninen, Phys. Rev. B **31**, 3486 (1985).

<sup>7</sup>W. Ekardt, Phys. Rev. B **31**, 6360 (1985).

<sup>8</sup>A. Hintermann and M. Manninen, Phys. Rev. B **27**, 7262 (1983).

<sup>9</sup>D. E. Beck, Solid State Commun. **49**, 381 (1984).

<sup>10</sup>W. Ekardt, Phys. Rev. B **29**, 1558 (1984).

<sup>11</sup>A. Zangwill and P. Soven, Phys. Rev. A **21**, 1561 (1980).

<sup>12</sup>M. J. Stott and E. Zaremba, Phys. Rev. A **21**, 12 (1980).

- <sup>13</sup>D. Pines and P. Nozières, *Theory of Quantum Liquids* (Benjamin, New York, 1966).
- <sup>14</sup>J. E. Inglesfield and E. Wikborg, *Solid State Commun.* **14**, 661 (1974).
- <sup>15</sup>G. D. Mahan, *Phys. Rev. A* **22**, 1780 (1980).
- <sup>16</sup>A. Liebsch, *Phys. Rev. Lett.* **54**, 67 (1985).
- <sup>17</sup>N. D. Lang and W. Kohn, *Phys. Rev. B* **3**, 1215 (1971).
- <sup>18</sup>W. D. Knight, K. Clemenger, W. A. de Heer, and W. A. Saunders, *Phys. Rev. B* **31**, 2539 (1985).
- <sup>19</sup>The alert reader will notice that  $q^{\text{cr}}$  of the random-phase approximation (RPA) is used for the TDLDA. We think this is allowed because, first, TDLDA and RPA are not so different and, second, we only try to get a hint at which  $l$  value the collective surface motion is expected to break down.